JOURNAL OF MATERIALS SCIENCE **38** (2003) 953–958

Influence of various divalent impurities on dislocation density in KCl:Mg^{2+}, Ca^{2+}, Sr^{2+} or Ba^{2+} single crystals

Y. KOHZUKI
Faculty of Engineering, Kanazawa University, Kodatsuno 2-40-20, Kanazawa 920-8667, Japan

Single crystals of nominally pure KCl and KCl doped with Mg^{2+}, Ca^{2+}, Sr^{2+} or Ba^{2+} were deformed by compression at 77–254 K; during the tests strain-rate cycling was conducted in association with ultrasonic oscillation. The data were analyzed in terms of strain-rate sensitivity ($(\Delta\tau'/\Delta\ln\dot{\varepsilon})$) versus stress decrement ($\Delta\tau$). The curve for KCl doped with the divalent impurities has two bending points and two plateau regions. It is proposed that the variation of strain-rate sensitivity at the second plateau place on the curve with shear strain ($\Delta(\Delta\tau'/\Delta\ln\dot{\varepsilon})/\Delta\varepsilon$) is due to a change in forest dislocation density with shear strain. The forest dislocation density for the specimens seemed to increase by the divalent additions in the compression test on account of the jogs on the screw dislocations. It depended on the concentration of impurities and also on the size of impurity in the specimens at a given temperature. Unfortunately, it was not possible to determine whether a change in the size of impurity influences mobile dislocation density, ρ, from the values of $\Delta\rho/\Delta\tau'$ for KCl doped with Ca^{2+}, Sr^{2+} or Ba^{2+}. © *2003 Kluwer Academic Publishers*

1. Introduction

The measurement of dislocation density in a crystal has been carried out by the etch pit technique. However, it is difficult to resolve the individual etch pits for high dislocation density. X-ray topography has also been used, but there is lack of resolution in the photograph for large deformation. Therefore, the specimens for these methods were limited to low dislocation density. Although the electron microscopy could be used to detect dislocations, it provided the information for a thin specimen but not for bulk.

The information on the interaction between a mobile dislocation and impurities has been obtained from the relative position of strain-rate sensitivity versus stress decrement curves due to oscillation for KCl doped with divalent [1–3] or monovalent impurities [4, 5]. The curve for KCl doped with the divalent impurities had two bending points and two plateau regions [1, 3]. Fig. 1 shows the curve for KCl:Ba^{2+} (0.050 mol% in the melt). The relative positions of the curves reflected the influence of ultrasonic oscillation on the dislocation motion on the slip plane containing many impurities and a few forest dislocations [1–4]. Furthermore, it was considered that the variation of strain-rate sensitivity at the second plateau place on the curve with shear strain, $\Delta(\Delta\tau'/\Delta\ln\dot{\varepsilon})/\Delta\varepsilon$, indicates a change in forest dislocation density with shear strain [6]. In this paper, it is investigated in more detail whether the forest dislocation density is influenced by divalent impurities in KCl during plastic deformation. This means seems useful until the dislocation density is below about 10^{10} cm^{-2}. The mobile dislocation density for the specimens is also considered. KCl is an excellent material for an investigation of mechanical strength, since pure or doped KCl single crystals are readily available and a large number of investigations on the mechanical properties have been made with the crystals [7–12].

2. Experimental procedure

The single crystals used in this study were nominally pure KCl and KCl doped with Mg^{2+} (0.035 mol% in the melt), Ca^{2+} (0.035 and 0.065 mol% in the melt), Sr^{2+} (0.035, 0.050 and 0.065 mol% in the melt) or Ba^{2+} (0.050 and 0.065 mol% in the melt) as divalent impurities. The concentration of divalent impurities, c, in the specimens was determined by dielectric loss measurement. The measurement at 393 K for KCl:Sr^{2+} has already been described in detail [2]. The size of the specimens was $5 \times 5 \times 15$ mm^3. The specimens were annealed at 973 K for 24 h and were cooled to room temperature at the rate of 40 K h^{-1} in order to reduce the dislocation density. Furthermore, the specimens were held at 673 K for 30 min and then quenched to room temperature immediately before a test in order to disperse the impurities. The specimens were deformed by compression along the ⟨100⟩ axis at temperatures from 77–254 K and an ultrasonic oscillatory stress was applied by a resonator in the same direction as the compression. Then, the stress drop due to superposition of oscillatory stress during plastic deformation is $\Delta\tau$. A strain-rate cycling between 1.1×10^{-5} and 5.5×10^{-5} s^{-1} was carried out keeping the stress amplitude constant. The stress change due to the strain-rate cycling is $\Delta\tau'$ and

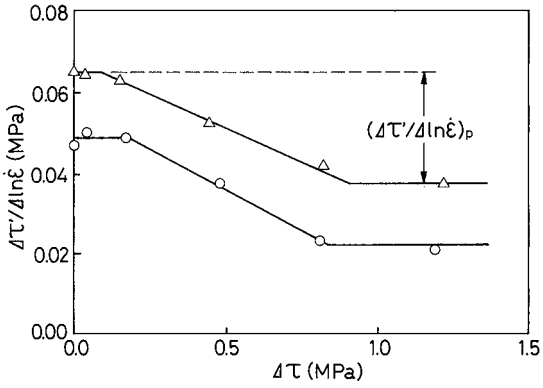

Figure 1 Strain-rate sensitivity versus stress decrement curve for KCl:Ba^{2+} (0.050 mol%) at 178 K. ε: (○) 10%, (△) 13%. $(\Delta\tau'/\Delta\ln\dot{\varepsilon})_p$ is assumed to be the strain-rate sensitivity due to impurities.

$\Delta\tau'/\Delta\ln\dot{\varepsilon}$ was used as a measure of the strain-rate sensitivity. A schematic illustration of the apparatus devised by Ohgaku was shown in a previous paper [1].

3. Results and discussion

3.1. Influence of the divalent impurities on the forest dislocation density

3.1.1. Influence of the divalent impurities on the forest dislocation density in different plastic deformation regions of stress versus strain curve

Three-stage strain hardening has been clearly established as the characteristic behavior of single crystals of rock salt structure, deforming predominantly by single glide [13]. It is also observed for KCl [6, 14, 15] and KCl:Mg^{2+}, Ca^{2+}, Sr^{2+} or Ba^{2+} single crystals. The three-stage of KCl:Ba^{2+} is illustrated in Fig. 2, which is generally denoted by stage I, II, and III. The relation between temperature and $\Delta(\Delta\tau'/\Delta\ln\dot{\varepsilon})/\Delta\varepsilon$ in stage I and stage II of stress versus strain curve was investigated for the five kinds of specimens. The results are shown in Fig. 3 for KCl:Mg^{2+} and KCl, Fig. 4 for KCl:Ca^{2+} and KCl, Fig. 5a and b for KCl:Sr^{2+} and KCl, and Fig. 6 for KCl:Ba^{2+} and KCl respectively. The full lines in these figures are to guide the reader's eye. Similar phenomena as described previously for KCl doped with monovalent impurities [6] are also observed for KCl doped with divalent additions. They are the following two phenomena. First, $\Delta(\Delta\tau'/\Delta\ln\dot{\varepsilon})/\Delta\varepsilon$ in stage II is

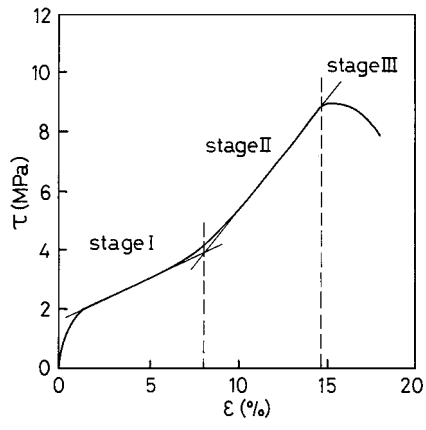

Figure 2 Stress versus strain curve for KCl:Ba^{2+} (0.050 mol%) at 145 K.

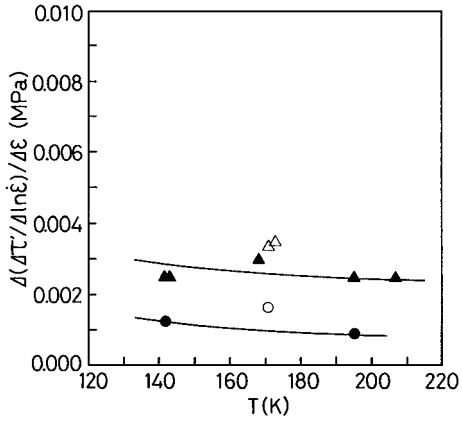

Figure 3 Dependence of $\Delta(\Delta\tau'/\Delta\ln\dot{\varepsilon})/\Delta\varepsilon$ on the temperature for KCl:Mg^{2+} (0.035 mol%) and KCl in the different plastic deformation regions: (○) KCl:Mg^{2+} and (●) KCl in stage I; (△) KCl:Mg^{2+} and (▲) KCl in stage II.

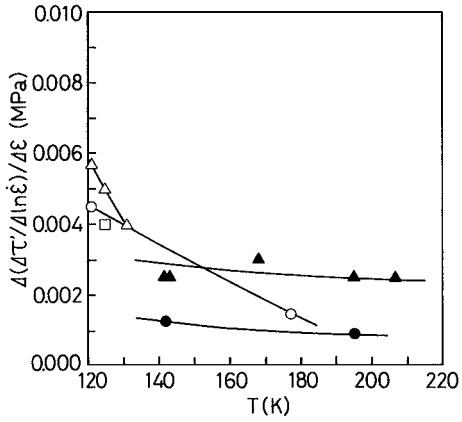

Figure 4 Dependence of $\Delta(\Delta\tau'/\Delta\ln\dot{\varepsilon})/\Delta\varepsilon$ on the temperature for KCl:Ca^{2+} and KCl in the different plastic deformation regions: (○) KCl:Ca^{2+} (0.035 mol%), (□) KCl:Ca^{2+} (0.065 mol%) and (●) KCl in stage I; (△) KCl:Ca^{2+} (0.035 mol%) and (▲) KCl in stage II.

larger than that in stage I at a given temperature for all of the specimens. This suggests that the forest dislocation density for the specimens slightly increases with the shear strain in stage I and then rapidly increases in stage II. Secondly, the $\Delta(\Delta\tau'/\Delta\ln\dot{\varepsilon})/\Delta\varepsilon$ in stage I and stage II increases with decreasing temperature for KCl and KCl doped with Ca^{2+}, Sr^{2+} or Ba^{2+}. From the second phenomenon, the forest dislocation density at a given shear strain in stage I and stage II may be considered to increase with decreasing temperature when the specimens are deformed in compression test. The dislocation density on the surface of Ge single crystals also increased with decreasing temperature in the same deformation region of stage I and stage II during the tensile test [16]. In Figs 3–6, we can additionally observe that the value of $\Delta(\Delta\tau'/\Delta\ln\dot{\varepsilon})/\Delta\varepsilon$ for KCl doped with the divalent impurities is markedly larger as compared with that for KCl in stage I and stage II. As the divalent impurities in KCl increase $\Delta(\Delta\tau'/\Delta\ln\dot{\varepsilon})/\Delta\varepsilon$, it may be deduced that the forest dislocation density increases due to the divalent impurities. Dislocations multiply through the process of double cross-slip in LiF [17]. It may be predicted that the addition of divalent impurities influences the ability of cross slip or the frequency of cross slips. If it happens in KCl doped with the divalent impurities, the ability of dislocation multiplication will

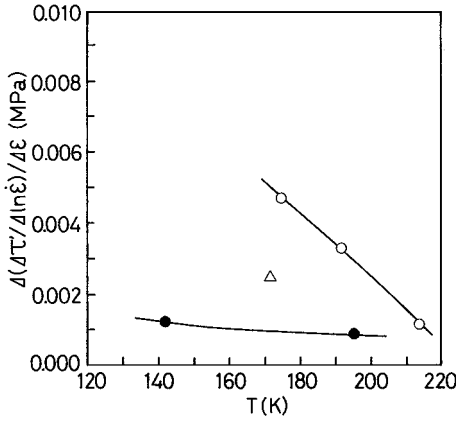

(a)

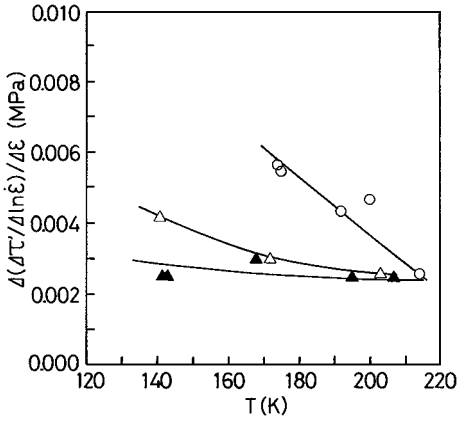

(b)

Figure 5 Dependence of $\Delta(\Delta\tau'/\Delta\ln\dot{\varepsilon})/\Delta\varepsilon$ on the temperature for KCl:Sr^{2+} and KCl in the different plastic deformation regions: (a) (△) KCl:Sr^{2+} (0.035 mol%), (○) KCl:Sr^{2+} (0.050 mol%) and (●) KCl in stage I; (b) (△) KCl:Sr^{2+} (0.035 mol%), (○) KCl:Sr^{2+} (0.050 mol%) and (▲) KCl in stage II.

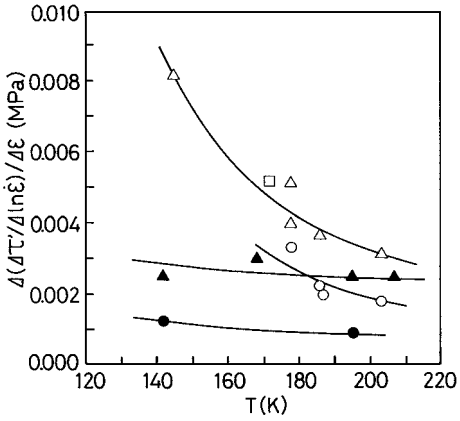

Figure 6 Dependence of $\Delta(\Delta\tau'/\Delta\ln\dot{\varepsilon})/\Delta\varepsilon$ on the temperature for KCl:Ba^{2+} and KCl in the different plastic deformation regions: (○) KCl:Ba^{2+} (0.050 mol%) and (●) KCl in stage I; (△) KCl:Ba^{2+} (0.050 mol%), (□) KCl:Ba^{2+} (0.065 mol%) and (▲) KCl in stage II.

be changed by the impurities. When a dislocation in ionic crystal moves under an applied stress, the screw segments can cross slip, especially if they become held up by an obstacle [18]. The segments that then lie in the cross-slip plane have edge character and cannot slip conservatively in the direction of the Burgers vector. Hence these jogs on screw dislocations, which are produced by the cross slips, act as pinning points tending to restrain the forward motion of the screw segments [18]. The pinning points may act as dislocation sources. Consequently, the forest dislocation density would depend on the divalent additions. Etch pit technique revealed that there are screw dislocations on all possible active slip planes in a crystal of rock salt structure [19]. The ability of cross slip is generally governed also by the Peierls stress in the cross-slip plane. This, however, is not taken into account in this study, because the mobile dislocations in KCl are impeded by it below several tens K [11, 20].

The screw segments can cross slip with the aid of thermal fluctuations, where the activation volume is approximately 10 to 10^2 b^3 [21], so that the frequency of cross slips seems to be higher at high temperature. This may lead to multiply the forest dislocation density, i.e. $\Delta(\Delta\tau'/\Delta\ln\dot{\varepsilon})/\Delta\varepsilon$. But the results shown in Figs 3–6 are contrary to the above expectation. It may be considered that the screw segments can more easily move forward by breaking away from the impurities on the slip plane, where the activation volume seems to be on the order of 10^2 b^3 [22], rather than the cross slips with increasing temperature.

3.1.2. Influence of the concentration of divalent impurities on the forest dislocation density

In Figs 5a, b and 6, $\Delta(\Delta\tau'/\Delta\ln\dot{\varepsilon})/\Delta\varepsilon$ at a given temperature increases with the concentration of divalent impurities. That is, the forest dislocation density becomes high with the concentration of divalent impurities in the compression test. Similar result has been found for NaC1:Ca^{2+} single crystals at the beginning of deformation ($\varepsilon = 1\%$, $T = 222.5$ K) [23]. As can be seen from Fig. 5a and b, this is clear in the two stages for KCl:Sr^{2+} and further becomes more clearly at low temperature. The mobility of jogs on the screw dislocations, where the activation volume for non-conservative motion of jogs is approximately 10^2 to 10^4 b^3 [21], would become low with the addition of divalent impurities. This may give rise to multiply jogs on the screw dislocations with increasing the impurity concentration. Therefore, the dislocation density seems to be higher with the concentration in accordance with the dislocation behavior mentioned in the preceding section. Unfortunately, $\Delta(\Delta\tau'/\Delta\ln\dot{\varepsilon})/\Delta\varepsilon$ in stage I for KCl:Ba^{2+} (0.065 mol% in the melt) could not be derived on the basis of strain-rate sensitivity versus stress decrement curves. In Fig. 4, no difference between $\Delta(\Delta\tau'/\Delta\ln\dot{\varepsilon})/\Delta\varepsilon$ for KCl:Ca^{2+} (0.035 mol% in the melt) and for KCl:Ca^{2+} (0.065 mol% in the melt) can be observed in stage I at 125 K. This is because the concentration of divalent impurities in KCl:Ca^{2+} (0.035 mol% in the melt), of which c is determined to be 43.1 p.p.m., is nearly equal to that for KCl:Ca^{2+} (0.065 mol% in the melt), of which c is 43.5 p.p.m.

3.1.3. Influence of the size of divalent impurity on the forest dislocation density

It was investigated whether the forest dislocation density is influenced by a change in the size of

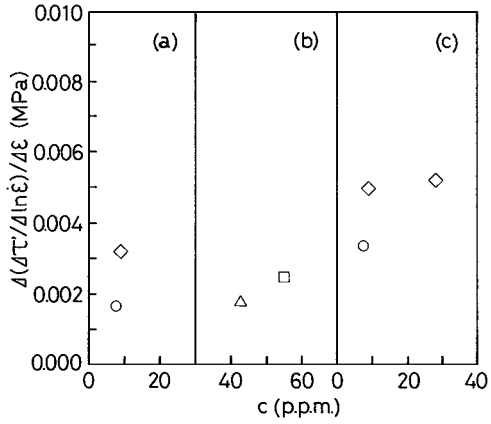

Figure 7 $\Delta(\Delta\tau'/\Delta\ln\dot{\varepsilon})/\Delta\varepsilon$ for (○) KCl:Mg^{2+}, (△) KCl:Ca^{2+}, (□) KCl:Sr^{2+} and (◇) KCl:Ba^{2+} at various conditions: (a) stage I and 171 K, (b) stage I and 172 K and (c) stage II and 171 K. The concentration of divalent impurities, c, is obtained by dielectric loss measurement.

divalent impurity in the specimens. Fig. 7a–c shows the $\Delta(\Delta\tau'/\Delta\ln\dot{\varepsilon})/\Delta\varepsilon$ at almost the same concentration of divalent impurities around 171 K. The $\Delta(\Delta\tau'/\Delta\ln\dot{\varepsilon})/\Delta\varepsilon$ in Fig. 7a and b is in stage I and that in Fig. 7c is in stage II. $\Delta(\Delta\tau'/\Delta\ln\dot{\varepsilon})/\Delta\varepsilon$, i.e. the forest dislocation density, in the two stages increases with the size of divalent addition. Therefore, it is considered that the frequency of cross slips grow higher when the divalent cation size approaches to the K^+ ionic size at the temperature.

3.2. Influence of the divalent impurities on mobile dislocation density

In this section, it was investigated whether the difference in size of divalent impurity influences mobile dislocation density for KCl doped with Ca^{2+}, Sr^{2+} or Ba^{2+}. As the mobile dislocation density cannot be determined directly, the density was investigated from pre-exponential factor, $\dot{\varepsilon}_0$, by reason of the description [23]: the most probable variable in $\dot{\varepsilon}_0$ is due to the density of mobile dislocations.

If the interaction between a dislocation and an impurity can be approximated to the Fleischer's model [24] taking account of the Friedel relation [25], the Gibbs free energy, ΔG_0, for the breakaway of the dislocation from the impurity is calculated from the following equation [26]:

$$\partial\ln\dot{\varepsilon}/\partial\tau = \{2\Delta G_0/(3kT\tau_0)\}\left\{1-(T/T_c)^{1/2}\right\}^{-2} \times (T/T_c)^{1/2} + \partial\ln\dot{\varepsilon}_0/\partial\tau \quad (1)$$

where kT has the usual meaning, τ_0 is the effective shear stress due to the impurities at 0 K, T_c is the critical temperature T, at which the effective shear stress is zero. The model is hereafter termed the F–F. The results of Equation 1 are shown in Fig. 8a [27] for KCl:Ca^{2+}, b [26] for KCl:Sr^{2+}, and c [27] for KCl:Ba^{2+} respectively. In Fig. 8a–c, τ_0 is replaced by τ_{p0}. τ_{p0} is the effective shear stress due to impurities without thermal activation [1, 4] and is re-tabulated in Table I. In addition, the $\partial\ln\dot{\varepsilon}/\partial\tau$ in Equation 1 is represented by $(\Delta\ln\dot{\varepsilon}/\Delta\tau')_p$. The $(\Delta\tau'/\Delta\ln\dot{\varepsilon})_p$, which is given by

TABLE I Values of τ_{p0} for the F–F

Specimen	(mol% in the melt)	τ_{p0} (MPa)
KCl:Ca^{2+}	(0.035)	15.34 [27]
	(0.065)	14.11 [27]
KCl:Sr^{2+}	(0.035)	11.44 [26]
	(0.050)	25.47 [26]
	(0.065)	36.31 [26]
KCl:Ba^{2+}	(0.050)	5.34 [27]
	(0.065)	7.27 [27]

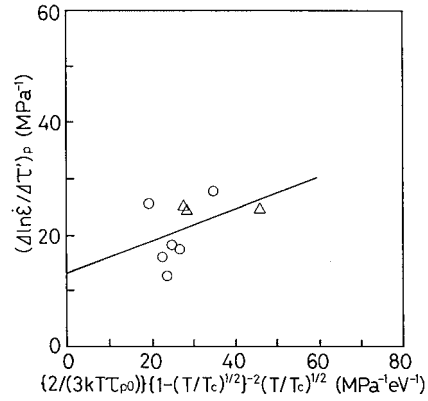

(a)

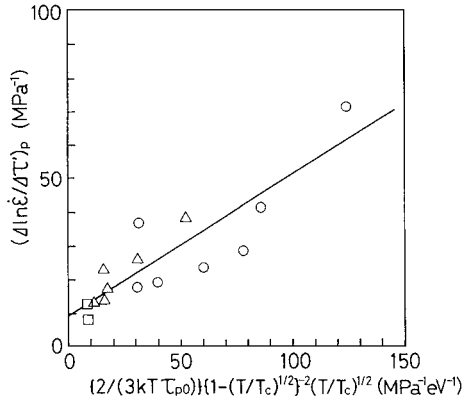

(b)

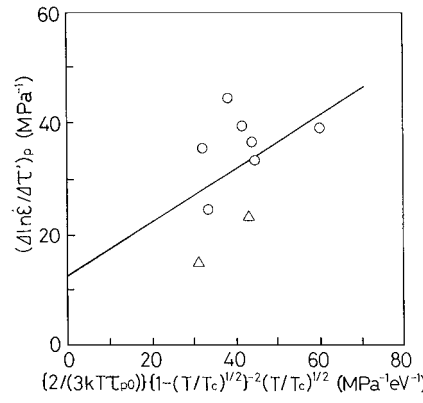

(c)

Figure 8 Linear plots of Equation 1 for (a) KCl:Ca^{2+} (○) 0.035 mol% and (△) 0.065 mol% [27], for (b) KCl:Sr^{2+} (○) 0.035 mol%, (△) 0.050 mol% and (□) 0.065 mol% [26] and for (c) KCl:Ba^{2+} (○) 0.050 mol% and (△) 0.065 mol% [27].

TABLE II Values of $\Delta \ln \dot{\varepsilon}_0/\Delta\tau'$

Specimen	$\Delta \ln \dot{\varepsilon}_0/\Delta\tau'$ (MPa^{-1})
KCl:Ca^{2+}	13.1
KCl:Sr^{2+}	9.0
KCl:Ba^{2+}	12.5

the difference between strain-rate sensitivity at first plateau place and at second one on the strain-rate sensitivity versus stress decrement curve as presented in Fig. 1, is assumed to be the strain-rate sensitivity due to impurities [2, 3, 5]. Accordingly, the $\partial \ln \dot{\varepsilon}_0/\partial\tau$ in Equation 1 can be represented by $\Delta \ln \dot{\varepsilon}_0/\Delta\tau'$. Then, the values of $\Delta \ln \dot{\varepsilon}_0/\Delta\tau'$, at which the solid lines intersect the ordinate in Fig. 8a–c, are given in Table II. $\dot{\varepsilon}_0$ is expressed by [28, 29]

$$\dot{\varepsilon}_0 = \rho b^2 \nu_D (L_0/L)^2 \tag{2}$$

where ρ is the density of mobile dislocations, b is the magnitude of the Burgers vector, ν_D is the Debye frequency, L_0 is the average spacing of impurities on the slip plane and L is the average length of dislocation segments at 0 K. The L may be given by the Friedel relation [25]:

$$L = \left\{2L_0^2 E/(\tau_0 b)\right\}^{1/3} \tag{3}$$

where E is the line tension of the dislocations and is calculated by μb^2. μ is the shear modulus at 0 K. Substituting Equation 3 in Equation 2, we find

$$\dot{\varepsilon}_0 = \rho \nu_D \left\{b^8 L_0^2 \tau_0^2 \big/ (2E)^2\right\}^{1/3} \tag{4}$$

Differentiating the natural logarithmic equation of Equation 4 with respect to the effective shear stress gives

$$\partial \ln \dot{\varepsilon}_0/\partial\tau = (\partial \ln\rho/\partial\tau) + 2/(3\tau_{p0}) \tag{5}$$

where τ_0 is replaced by τ_{p0}. Substituting the values of $\Delta \ln \dot{\varepsilon}_0/\Delta\tau'$ and τ_{p0} into Equation 5, $(\Delta \ln\rho/\Delta\tau')$ can be obtained for the three kinds of specimens. The results are listed in Table III. The values of $(\Delta\rho/\Delta\tau')$ are within stage II of stress versus strain curve, since almost all of the $(\Delta \ln \dot{\varepsilon}/\Delta\tau')_p$ in Fig. 8a–c are obtained on the basis of the strain-rate sensitivity versus stress decrement curve at the shear strain in stage II. However, $(\Delta \ln\rho/\Delta\tau')$ for KCl:Mg^{2+} could not be obtained according to the above-mentioned process, because the F–F seemed not to be appropriate for the interaction between a dislocation and the impurity in KCl:Mg^{2+} [27]. As given in Table III, no great difference of $(\Delta\rho/\Delta\tau')$ between the three kinds of specimens can be unfortunately discriminated on account of scattered the experimental data in Fig. 8a–c. The values of $(\Delta\rho/\Delta\tau')$ for the specimens, however, seem to be less than about 50 cm^{-2} MPa^{-1}.

TABLE III Values of $(\Delta\rho/\Delta\tau')$ at 0 K

Specimen	(mol% in the melt)	$(\Delta\rho/\Delta\tau')$ (cm^{-2} MPa^{-1})
KCl:Ca^{2+}	(0.035)	46.84
	(0.065)	46.65
KCl:Sr^{2+}	(0.035)	0.76
	(0.050)	0.79
	(0.065)	0.80
KCl:Ba^{2+}	(0.050)	23.68
	(0.065)	24.48

4. Conclusions

When the specimens are deformed in compression test, the following five phenomena are found on the basis of $\Delta(\Delta\tau'/\Delta \ln \dot{\varepsilon})/\Delta\varepsilon$.

1. The forest dislocation density for the specimens slightly increases with the shear strain in stage I and then rapidly increases in stage II.
2. The forest dislocation density increases with decreasing temperature at a given shear strain in stage I and stage II.
3. In the two stages, the forest dislocation density increases due to the divalent impurities in the specimens. It may be predicted that the addition of divalent impurities influences the ability of cross slip or the frequency of cross slips. We can image that the screw segments can cross slip under an applied stress, especially if they become held up by the impurity. These jogs on screw dislocations, which are produced by the cross slips, seem to act as pinning points tending to restrain the forward motion of the screw segments and further as dislocation sources. Consequently, the forest dislocation density would depend on the divalent additions.
4. The forest dislocation density becomes high with the concentration of the divalent impurities which may result in a large number of jogs on the screw dislocations. This becomes more clearly at low temperature.
5. When the divalent cation size approaches to the K^+ ionic size, the forest dislocation density increases around 171 K. This suggests that the frequency of cross slips grow higher with larger size of divalent impurity.

It is not found whether the change in the size of divalent impurity influences mobile dislocation density for the three kinds of specimens by reason of scattered the experimental data in Fig. 8a–c. However, $(\Delta\rho/\Delta\tau')$ in stage II seems to be less than about 50 cm^{-2} MPa^{-1} in the compression test.

References

1. Y. KOHZUKI, T. OHGAKU and N. TAKEUCHI, *J. Mater. Sci.* **28** (1993) 3612.
2. *Idem., ibid.* **28** (1993) 6329.
3. *Idem., ibid.* **30** (1995) 101.
4. T. OHGAKU and N. TAKEUCHI, *Phys. Status Solidi* (a) **134** (1992) 397.
5. Y. KOHZUKI, *J. Mater. Sci.* **33** (1998) 5613.
6. *Idem., ibid.* **35** (2000) 2273.
7. M. L. GREEN and G. ZYDZIK, *Scripta Metall.* **6** (1972) 991.
8. G. Y. CHIN, L. G. VAN UITERT, M. L. GREEN and G. ZYDZIK, *ibid.* **6** (1972) 475.
9. J. R. HOPKINS, J. A. MILLER and J. J. MARTIN, *Phys. Status Solidi* (a) **19** (1973) 591.
10. J. J. GILMAN, *J. Appl. Phys.* **45** (1974) 508.

11. T. KATAOKA, T. UEMATSU and T. YAMADA, *Jpn. J. Appl. Phys.* **17** (1978) 271.
12. M. T. SPRACKLING, "The Plastic Deformation of Simple Ionic Crystals," edited by A. M. Alper, J. L. Margrave and A. S. Nowick (Academic Press, London, 1976).
13. *Idem., ibid.* p. 203.
14. T. H. ALDEN, *Trans. Met. Soc. AIME* **230** (1964) 649.
15. L. A. DAVIS and R. B. GORDON, *J. Appl. Phys.* **40** (1969) 4507.
16. K. KOJIMA and K. SUMINO, *Cryst. Latt. Defects* **2** (1971) 147.
17. J. J. GILMAN and W. G. JOHNSTON, *Solid State Physics* **13** (1962) 147.
18. M. T. SPRACKLING, "The Plastic Deformation of Simple Ionic Crystals," edited by A. M. Alper, J. L. Margrave and A. S. Nowick (Academic Press, London, 1976) p. 109.
19. *Idem.*, "The Plastic Deformation of Simple Ionic Crystals," edited by A. M. Alper, J. L. Margrave and A. S. Nowick (Academic Press, London, 1976) p. 195.
20. T. SUZUKI, *Oyo Buturi* **45** (1976) 447 (in Japanese).
21. H. CONRAD, *J. Metals* **16** (1964) 582.
22. M. SRINIVASAN and T. G. STOEBE, *J. Mater. Sci.* **8** (1973) 1567.
23. F. APPEL, *Phys. Status Solidi* (a) **61** (1980) 477.
24. R. L. FLEISCHER, *J. Appl. Phys.* **33** (1962) 3504.
25. J. FRIEDEL, "Dislocations" (Pergamon Press, Oxford, 1964) p. 224.
26. Y. KOHZUKI, *J. Mater. Sci.* **35** (2000) 3397.
27. Y. KOHZUKI and T. OHGAKU, *ibid.* **36** (2001) 2009.
28. K. SUMINO, "Plasticity of Crystals" (Maruzen, Tokyo, 1977) p. 356 (in Japanese).
29. *Idem., Japan Inst. Metals* **11** (1972) 31 (in Japanese).

Received 16 April
and accepted 30 October 2002